ARTICLE

Check for updates

# Decadal increase in groundwater inorganic carbon concentrations across Sweden

Marcus Klaus [1,2 ✉]

Groundwater is one of the largest continental carbon reservoirs and tightly linked to globally important carbon fluxes such as uptake on land, degassing from inland waters and delivery to oceans. Despite emerging evidence that these fluxes are sensitive to environmental changes, long-term carbon dynamics in groundwater remain widely unknown. Here I show that dissolved inorganic carbon and carbon dioxide concentrations in groundwater, calculated from environmental monitoring data (e.g. alkalinity, pH), have increased on average by 28% and 49%, respectively, across Sweden during 1980–2020. I attribute the observed changes mainly to a partial recovery from atmospheric sulfate deposition and associated shifts in weathering pathways, but also to enhanced soil respiration. The results highlight previously neglected long-term and large-scale dynamics in groundwater carbon cycling. These dynamics should be included in carbon cycle models for accurate evaluations and predictions of the effects of environmental changes on landscape and global carbon stocks and fluxes.

[1] Department of Forest Ecology and Management, Swedish University of Agricultural Sciences, Umeå, Sweden. [2] Department of Ecosystem Trace Gas Exchange, Global Change Research Institute of the Czech Academy of Sciences, Brno, Czech Republic. ✉email: marcus.klaus@posteo.net

Globally, groundwater stores around 1400 Pg carbon (C), similar as soils and twice as much as the atmosphere[1]. Groundwater is tightly linked to C dynamics in the atmosphere because it receives C mainly through plant uptake and subsequent respiration, releases C to surface waters where a large proportion of it is emitted back to the atmosphere, or delivers C to oceans[2,3]. Therefore, even small changes in the C flux between groundwater and atmosphere could have large impacts on atmospheric carbon dioxide ($CO_2$) concentrations[1]. Dissolved C also regulates key characteristics and processes in aquatic ecosystems such as pH and metabolism[4]. Despite this potential importance, groundwater C dynamics are usually neglected in C budgets and models[2,5,6], which may lead to biased evaluations and predictions of landscape and global C fluxes with implications for aquatic ecosystem functioning, climate change predictions and the development of soil C sequestration activities.

The C export from land to surface waters has doubled globally since 1750 due to anthropogenic perturbations[7]. Ongoing climate and land use change may mobilize fossil C stored in the subsurface, which would cause further climate warming and aquatic ecosystem perturbations[8,9]. These estimates and predictions were mainly based on observations or modeling of surface water C dynamics, but for a rigorous evaluation of the underlying mechanisms, direct estimates of groundwater C dynamics are needed. Only few studies have examined groundwater C dynamics at large spatiotemporal scales relevant for landscape and global C cycling assessments. Based on global groundwater observations, a recent study predicted dissolved organic carbon (DOC) in groundwater to increase due to climate and land use changes[10]. However, groundwater C typically mainly consists of dissolved inorganic carbon (DIC), i.e. the sum of $CO_2$, bicarbonate ($HCO_3^-$), and carbonate ($CO_3^{2-}$)[11–13]. The relative proportion of these species is driven by pH dependent equilibrium reactions. Studies on long-term dynamics or large-scale patterns of groundwater DIC are rare and analyses of long-term DIC dynamics over large scales are lacking[11,13]. Current research is therefore missing a potentially important component of the C cycle with implications for the magnitude, origin, and fate of land-atmosphere C fluxes.

Groundwater DIC can be expected to be highly sensitive to anthropogenic activities[7,13]. For example, increased temperature, atmospheric $CO_2$ concentration or nutrient availability can stimulate plant growth, soil respiration and hence groundwater C uptake and weathering[13,14]. Increased precipitation may further enhance C leaching[15], whereas drought or human groundwater extraction may decrease C sequestration[16]. Expansion of agricultural and urban areas increases soil disturbance and input of substances that can fuel weathering or organic C decomposition[17]. Perhaps most importantly, atmospheric deposition of strong acids originating from air pollution changes the uptake and mobilization of C species through weathering and carbonate equilibrium reactions[17,18]. Under pristine conditions, weathering in most soils converts carbonic acid to $HCO_3^-$. In the presence of nitric or sulfuric acids, however, weathering of non-carbonate rocks would not generate any $HCO_3^-$. Acid inputs, if not neutralized by the groundwater buffering system, may also shift the carbonate equilibrium towards more $CO_2$. While there is compelling evidence that atmospheric acid deposition has impacted the carbonate system over decadal time scales in many surface waters across the globe[17,19–21], studies in groundwater are lacking.

Here, I report significant large-scale decadal increases in groundwater molar DIC and $CO_2$ concentrations across Sweden. I attribute these trends to a partial recovery from historic anthropogenic acid deposition and increased soil respiration. Based on the results, I discuss likely scenarios for future conditions and for other regions worldwide, and discuss the need for a closer integration of groundwater into C cycle and ecosystem models. My findings are based on groundwater chemistry data collected in a certified and standardized manner by the Swedish national environmental monitoring program. Measured pH, alkalinity and water temperature allowed me to calculate DIC and $CO_2$ using a carbonate speciation model. The dataset includes 12,154 observations from 207 sites collected since 1962. Here, I focus on 5742 observations from 55 sites (25 wells and 30 springs) with continuous monitoring during 1980–2020. The sites are representative for the Swedish forest dominated landscape and cover a wide range of latitudes from the temperate to the subarctic biome (55–68°N), well depths (2–231 m), bedrock mineral composition (silicates ($n = 41$), carbonates ($n = 14$)), aquifer types (unconfined ($n = 40$), confined ($n = 15$)) and water chemistry (Table 1). The variety of sites provides valuable geographical and hydrogeological context for discussions on the potential drivers of the observed DIC and $CO_2$ trends.

## Results and discussion

**Decadal increase in groundwater DIC.** Groundwater DIC and $CO_2$ increased significantly across Sweden during 1980–2020. DIC and $CO_2$ increased on average by 0.09 (0.06–0.13) mg C $L^{-1}$ $yr^{-1}$ and 0.06 (0.04–0.09) mg C $L^{-1}$ $yr^{-1}$, respectively (Fig. 1, numbers in parentheses give 95% confidence intervals based on uncertainties in raw data). Relative to median concentrations, the increase was 0.69 (0.42–0.97)% $yr^{-1}$ and 1.20 (0.73–1.66)% $yr^{-1}$, which corresponds to a total increase during the study period of 28 (17–40)% and 49 (30–68)%, respectively. The relative rate increase in groundwater $CO_2$ was about twice as large as in the atmosphere[22]. The DIC and $CO_2$ trends were robust even when transforming DIC and $CO_2$ concentrations to account for the composition of other major constituents such as base cations and acid anions (Supplementary Methods 2, Supplementary Fig. 1e, f). Across Sweden, significant increasing trends outnumbered other trends. DIC and $CO_2$ increased significantly ($p < 0.05$) in 58% (42–75%) and 60% (35–71%) and decreased in 5% (0–15%) and 2% (0–25%) of all sites, respectively. DIC and $CO_2$ trends did not vary significantly with geographical or hydrogeological settings (latitude, well depth, bedrock mineral composition, aquifer type), but DIC increases tended to be lower in deeper wells ($p = 0.048$ (0.015–0.137) and at higher latitudes ($p = 0.057$ (0.016–0.170, Supplementary Table 3). The trends in the dataset of 55 sites were consistent with the larger dataset that includes up to 207 sites with ≥10 years of data (Supplementary Fig. 2).

The main input variables to DIC calculations, alkalinity and pH, shifted markedly during the study period. Alkalinity, here expressed as bicarbonate alkalinity ($HCO_3^-$, see methods), remained unchanged until 2000 but increased afterwards by 0.03 (0.02–0.06) mg C $L^{-1}$ $yr^{-1}$, as a mean among all sites (Fig. 2a, c). Conversely, pH declined until 2000 by 0.008 (0.005–0.014) $yr^{-1}$ and remained at low levels afterwards (Fig. 2b, d). The pH decline corresponded to an increase in $H^+$ ion activity of 2.9 (1.7–4.2)% $yr^{-1}$. Changes in $HCO_3^-$ and pH were detected across the whole range of sites covering pH of 5.15–8.10 and $HCO_3^-$ of 0.4–64.1 mg C $L^{-1}$ (Fig. 2e). Most of the sites exhibited a significant break point in linear trends for pH and $HCO_3^-$ (64% and 69%, respectively), clustering around the year 2000 (Supplementary Fig. 3). Hence, 2000 divides the study period into distinct regimes with different primary DIC drivers. As inferred from the C speciation model, the DIC increase could be mainly explained by increasing $CO_2$ resulting from declining pH and stable $HCO_3^-$ during 1980–2000, and by the $HCO_3^-$ increase and stable pH during 2000–2020 (Supplementary Fig. 4).

**Table 1 Physicochemical and geographical characteristics of the studied groundwater sampling sites.**

| Variable | Unit | Mean | SD | Min | Max | Mean $n_{obs}$ |
|---|---|---|---|---|---|---|
| Latitude | ° | 60.46 | 3.63 | 55.39 | 68.36 | – |
| Longitude | ° | 15.94 | 2.78 | 11.50 | 21.78 | – |
| Well depth | m | 27.88 | 52.54 | 1.85 | 231 | – |
| pH | unitless | 6.10 | 0.76 | 5.16 | 8.08 | 104 |
| $Ca^{2+}$ | mEq $L^{-1}$ | 1.23 | 1.59 | 0.05 | 6.86 | 103 |
| $Mg^{2+}$ | mEq $L^{-1}$ | 0.25 | 0.27 | 0.02 | 1.11 | 104 |
| $K^+$ | mEq $L^{-1}$ | 0.04 | 0.03 | 0.01 | 0.15 | 104 |
| $Na^+$ | mEq $L^{-1}$ | 0.33 | 0.70 | 0.05 | 5.21 | 104 |
| $HCO_3^-$ | mEq $L^{-1}$ | 1.24 | 1.53 | 0.03 | 5.34 | 101 |
| $Cl^-$ | mEq $L^{-1}$ | 0.25 | 0.30 | 0.02 | 1.65 | 104 |
| $NO_3^-$ | mEq $L^{-1}$ | 0.05 | 0.14 | 0.00 | 0.82 | 100 |
| $SO_4^{2-}$ | mEq $L^{-1}$ | 0.28 | 0.38 | 0.02 | 2.29 | 104 |
| $(Ca^{2+}+Mg^{2+}+K^++Na^+)/(HCO_3^-+Cl^-+NO_3^-+SO_4^{2-})$ | unitless | 1.01 | 0.08 | 0.44 | 1.11 | 95 |
| TOC | mg $L^{-1}$ | 2.32 | 2.03 | 0.60 | 10.90 | 95 |
| $O_2$ | mg $L^{-1}$ | 6.67 | 3.58 | 0.20 | 12.05 | 59 |
| $SiO_2$ | mg $L^{-1}$ | 11.50 | 4.46 | 3.41 | 23.53 | 90 |
| $NH_4^+$ | mEq $L^{-1}$ | 0.001 | 0.002 | 0.000 | 0.014 | 100 |
| T | °C | 6.21 | 1.76 | 2.20 | 10.80 | 95 |
| Water level | m | 1.35 | 1.28 | −0.18 | 5.27 | 95 |

Given are summary statistics among sampling sites ($n = 55$ for all variables except water table where $n = 15$) for geographic coordinates, pH, base cation ($Ca^{2+}$, $Mg^{2+}$, $Na^+$, $K^+$) and anion ($SO_4^{2-}$, $NO_3^-$, $Cl^-$, $HCO_3^-$) concentrations, cation-to-anion ratio, total organic carbon (TOC), dissolved oxygen ($O_2$), dissolved silica ($SiO_2$), ammonium ($NH_4^+$), groundwater temperature (T) and groundwater level. For water chemical and physical variables, these statistics are based on median values of time series for 1980–2020, except for TOC (2000–2020) because of incomplete data before 2000. Statistics on pH are based on back-transformed statistics of $H^+$ activity. Well depth refers to groundwater wells ($n = 25$) and excludes springs ($n = 30$). mean is arithmetic mean, SD is standard deviation, min is minimum, max is maximum. $n_{obs}$ is the total number of observations per site.
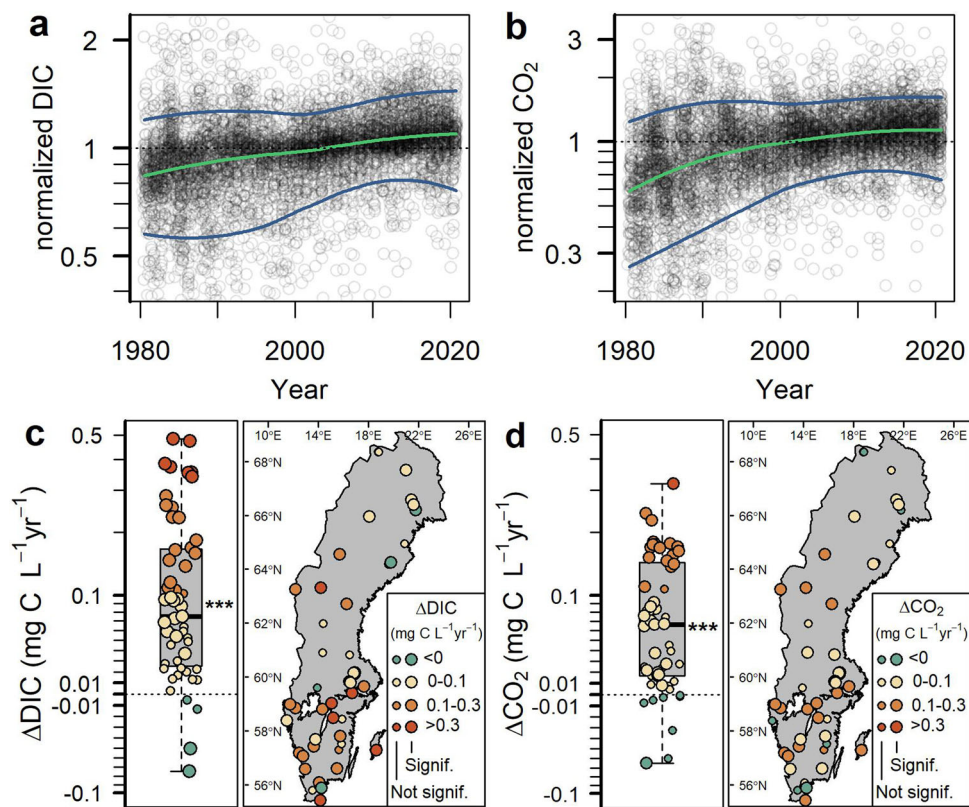


**Fig. 1 Trends in DIC and $CO_2$ concentrations across Swedish groundwater sampling sites during 1980−2020. a, b** Time series of DIC and $CO_2$, lumped for all sites and normalized to site-specific median values of 1980–2020. Lines show local quantile regressions (green = median, blue = 90% percentiles). Note that a few outliers are not shown. **c, d** Linear trends in DIC and $CO_2$ during 1980–2020 as boxplots, point estimates and maps. Boxplots show medians (thick line), interquartile ranges (box) and 1.5 times interquartile ranges (whiskers) and significance of two-tailed Student's t-test with null hypothesis h0: mean = 0 (***$p < 0.001$). Each circle represents one site. Circle size symbolizes significance of site-specific trends ($p < 0.05$). For statistical details, see Supplementary Table 1. For diagrams on DIC and $CO_2$ concentrations and trends relative to median DIC and $CO_2$ concentrations as well as relative to trends in the concentrations of major cations and anions, see Supplementary Fig. 1.
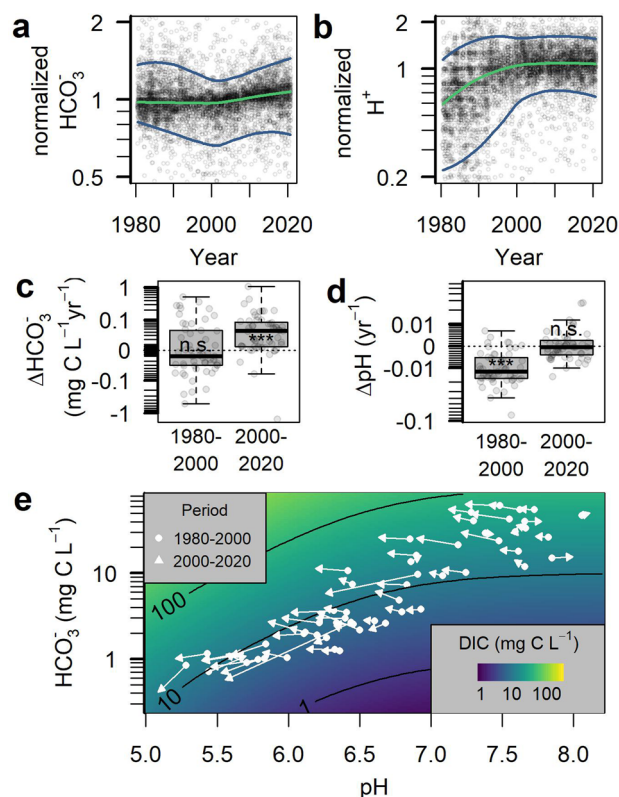
**Fig. 2 Shifting drivers of DIC during 1980−2020. a, b** Time series of $HCO_3^-$ and $H^+$ activity, respectively, lumped for all sites and normalized to site-specific median values of 1980-2020. Lines show local quantile regressions (green = median, blue = 90% percentiles). **c, d** The linear trend in $HCO_3^-$ and pH during 1980-2000 and 2000-2020 as boxplots. Boxplots show medians (thick line), interquartile ranges (box) and 1.5 times interquartile ranges (whiskers). Each circle in boxplots represents one site. Boxplots show significance levels of two-tailed Student's $t$-test with null hypothesis h0: mean = 0 (n.s. not significant, ***$p < 0.001$). **e** Site-specific median DIC as a function of $HCO_3^-$ and pH during 1980-2000 and 2000-2020. White lines show trajectories between the periods. DIC isoclines are based on the carbonate speciation model, using median water temperature and chemistry among sites. For statistical details, see Supplementary Table 1.

**Shifting weathering and acidification pathways drive DIC increase.** I mainly attribute the observed DIC increase to a partial recovery from historic atmospheric acid deposition and subsequent shifts in the sources and pathways of weathering and acidity. Acid deposition peaked in the 1970s and led to a historic decline in $HCO_3^-$ and pH throughout Sweden until ~1980[23]. The decline has partly reversed since 1980 due to emission control and subsequent deposition reductions of mainly sulfate $(SO_4^{2-})$[24,25]. This is reflected in an increase in $HCO_3^-$ (1.59 (0.69–2.71) µEq $L^{-1}$ $yr^{-1}$ as mean among sites) that was equivalent in magnitude to a decline in $SO_4^{2-}$ (1.36 (0.69–2.15) µEq $L^{-1}$ $yr^{-1}$) during 1980–2000 (Supplementary Table 2). Trends in $HCO_3^-$ correlated mainly and negatively with trends in acid anions $(SO_4^{2-}, NO_3^-)$ according to multivariate linear regressions (Supplementary Table 3, Supplementary Fig. 6). This tight association suggests recovery from acidification as the main driver of $HCO_3^-$. Here, changes in weathering dynamics play an important role. Overall weathering rates likely remained unchanged during the study period, because the most common base cations $(Ca^{2+}, Mg^{2+}, Na^+)$, accounting for 97% of the positive charges did not change (Supplementary Table 2, Supplementary Fig. 5).

However, the increase in $HCO_3^-$ was likely caused by shifts in weathering pathways, where contributions to weathering by sulfuric acid decreased relative to carbonic acid during the study period. This is indicated by two commonly used proxies, $SO_4^{2-}/(SO_4^{2-} + HCO_3^-)$ and $(Ca^{2+}+Mg^{2+})/HCO_3^-$, where ratios >0 and >1, respectively, indicate major contributions of sulfuric acid to weathering[17,18]. Swedish groundwater showed ratios of 0.31 (0.24–0.38) for $SO_4^{2-}/(SO_4^{2-} + HCO_3^-)$ and 1.49 (1.27–1.74) for $(Ca^{2+}+Mg^{2+})/HCO_3^-$ during 1980–2000 (Fig. 3a, b). Both ratios decreased significantly during 2000–2020, indicating decreased influence of sulfuric acid (Fig. 3c–f). The declines were largest towards lower latitudes where atmospheric $SO_4^{2-}$ deposition has been most pronounced[25], and were more negative in unconfined aquifers which are particularly sensitive to acidification[26] (Supplementary Fig. 7a−d, Supplementary Table 3). A $SO_4^{2-}$ decline could theoretically also be expected from lower pyrite oxidation due to rising groundwater levels, which was not found here (Supplementary Fig. 8a, Supplementary Table 2). Together, this stresses that recovery from atmospheric acid deposition has likely been the main cause for the observed $SO_4^{2-}$ and $HCO_3^-$ trends (Fig. 4).

An important precondition for the DIC rise was that $HCO_3^-$ and pH did not recover in concert from acid deposition. A parallel recovery in $HCO_3^-$ and pH would not necessarily imply an increase in DIC, because at least part of the additional $HCO_3^-$ would originate from consumption of $CO_2$ (Fig. 2e)[27]. Here, however, rising $HCO_3^-$ and falling pH collectively indicate both higher DIC and $CO_2$ (Supplementary Fig. 4). The absence of pH recovery is characteristic for areas with acid igneous bedrock and can be explained by slow weathering and exhausted acid buffering capacity[21,26,28,29]. This is supported here, because pH declines were more pronounced in relatively weakly buffered aquifers with silicate minerals in the reservoir bedrock, compared to more strongly buffered aquifers with carbonates (Supplementary Fig. 7e, Supplementary Table 3). A reduction in weathering and hence hydrogen ion consumption could theoretically lead to groundwater acidification. However, this is unlikely here, because weathering rates likely remained unchanged, as discussed above, and trends in major weathering products could explain only little of the observed $H^+$ trends among sites (Supplementary Table 3). An alternative driver could be enhanced acid input from trees due to increased removal of base cations from forest ecosystems as a result of increased forest harvest intensity[30]. This process can indeed at least in part explain the relatively slow pH recovery in Swedish forest soils[30]. Yet, it is unlikely to explain pH trajectories in groundwater, because it would imply a decrease in base cations[30], which was not observed here (Supplementary Table 2). Well-established theory[27] predicts that pH trends can be uncoupled from $HCO_3^-$ trends during different stages of acidification if processes other than weathering or ion exchange affect the charge balance in groundwater. For example, pH could drop in response to increased organic acidity. This is unlikely here, because organic acids contribute only little to acidity as indicated by low total organic carbon (TOC) concentrations (mean 2.3 mg $L^{-1}$, near equivalent to DOC[19]) and cation-to-anion ratios close to 1.0 with no significant trends (Table 1, Supplementary Table 2)[14]. Other potential drivers include episodic salt intrusions in coastal areas, and nitrification and nitrate-leaching, but in Sweden these effects are relatively short-lived or local[28,30]. Absence of overall trends in $Cl^-$ and $NO_3^-$ among the study sites further support this notion (Supplementary Table 2).

The most likely driver of the observed pH trends is increases in groundwater $CO_2$ (Fig. 1b)[24]. Through its effects on soil acidity and carbonate equilibria, $CO_2$ can affect pH and $HCO_3^-$ to the same quantitative extent as acid deposition and therefore alter or
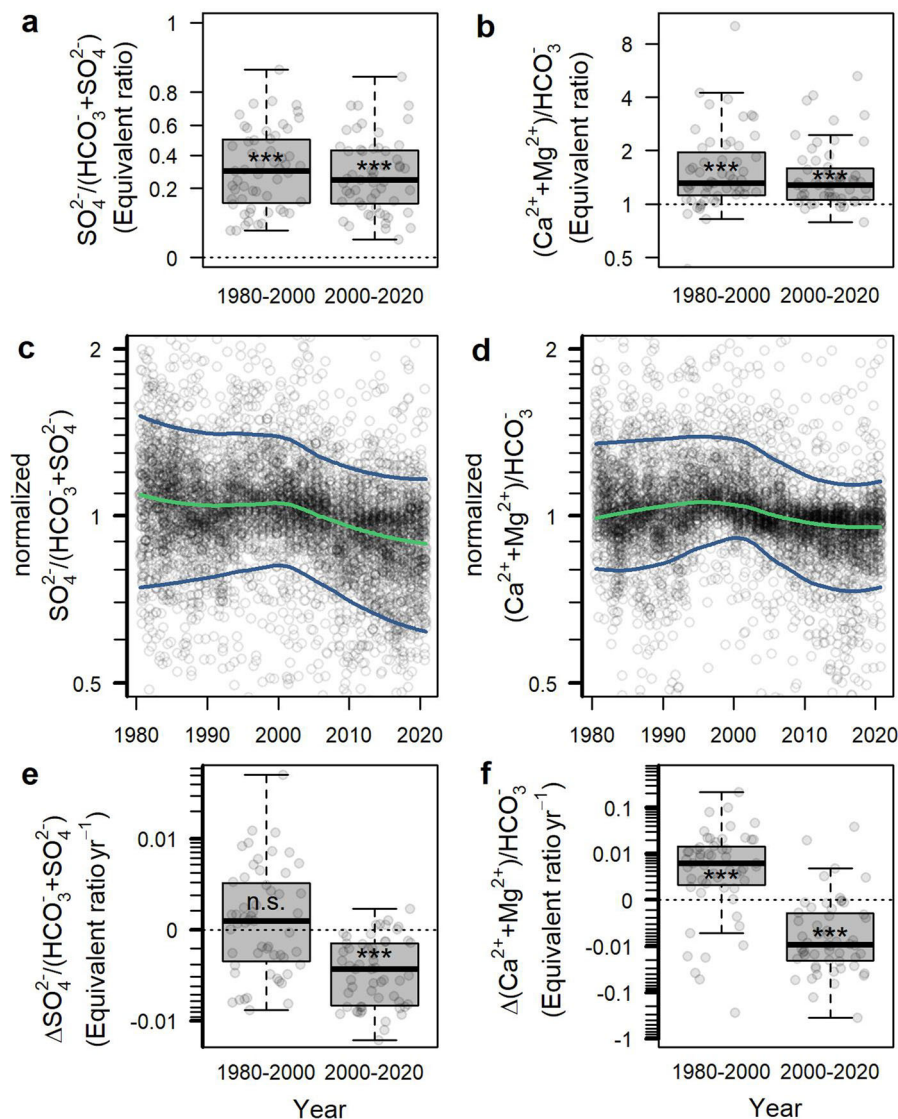
**Fig. 3 Recovery from acidification drives HCO$_3$− concentrations. a, b** Major influence of sulfuric acid on weathering as indicated by boxplots where SO$_4^{2-}$/(SO$_4^{2-}$ + HCO$_3^-$) > 0 and (Ca$^{2+}$+ Mg$^{2+}$)/HCO$_3^-$ > 1 for most sites. **c, d** Ongoing recovery from acidification as indicated by decreasing SO$_4^{2-}$/(SO$_4^{2-}$ + HCO$_3^-$) and (Ca$^{2+}$+ Mg$^{2+}$)/HCO$_3^-$ since 2000. The figures show time series observations, lumped for all sites and normalized to site-specific median values of 1980–2020. Lines show local quantile regression (green = median, blue = 90% percentiles). **e, f** Boxplots of trends in SO$_4^{2-}$/(SO$_4^{2-}$ + HCO$_3^-$) and (Ca$^{2+}$+Mg$^{2+}$)/HCO$_3^-$ during 1980–2000 and 2000–2020. Boxplots show medians (thick line), interquartile ranges (box), 1.5 times interquartile ranges (whiskers) and significance levels of two-tailed Student's *t*-test with null hypothesis h0: mean = 0 (**a**, **e**, **f**) or mean = 1 (**b**) (n.s. not significant, ***$p$ < 0.001). Each circle in boxplots represents one site. For statistical details, see Supplementary Table 1.

delay recovery from acid deposition[23,31,32]. Increased CO$_2$ may have resulted from enhanced soil respiration as caused by several mechanisms (Fig. 4). First, recovery from historic nitrogen deposition may have altered microbial activities, destabilized organic matter against decomposition, and enhanced C inputs to roots and hence increased heterotrophic or autotrophic soil respiration[33,34]. Nitrogen deposition has indeed decreased by ~35% across Sweden since the 1980s[25]. Even though NO$_3^-$ did not decline consistently among Swedish aquifers (Supplementary Table 2), study sites with the largest NO$_3^-$ decline showed the largest increase in H$^+$ and HCO$_3^-$ and hence DIC and CO$_2$ (Supplementary Fig. 6, Supplementary Table 3), possibly because of higher soil respiration and dissociation of more CO$_2$ in groundwater. Second, recovery from soil acidification may have increased the bioavailability of nutrients and enhanced primary productivity, root growth and microbial activity[35]. Swedish soils are indeed slowly recovering from these effects[28]. Another

consequence of this recovery is increased leaching of DOC acting as a potential substrate for CO$_2$ production[19,21]. While groundwater DOC trends cannot be fully evaluated here due to incomplete data before 2000, the increased DIC and constant HCO$_3^-$ during 1980–2000 may indicate substantial aerobic DOC decomposition[36]. Third, large-scale drivers other than atmospheric acid deposition must have contributed to the CO$_2$ rise in groundwater. This is because atmospheric deposition effects would be expected to decline with latitude, as discussed above, but CO$_2$ trends did not vary with latitude (Supplementary Table 3). One such alternative driver could be forest productivity. More productive forests produce more litter inputs and allocate more C to roots and therefore may yield higher soil respiration[37]. Forest productivity has indeed increased across Sweden by nearly 50% since the 1950s[38]. Fourth, rising atmospheric CO$_2$ concentrations may have led to increased respiration by roots and microbes[14]. Atmospheric CO$_2$ concentrations have indeed
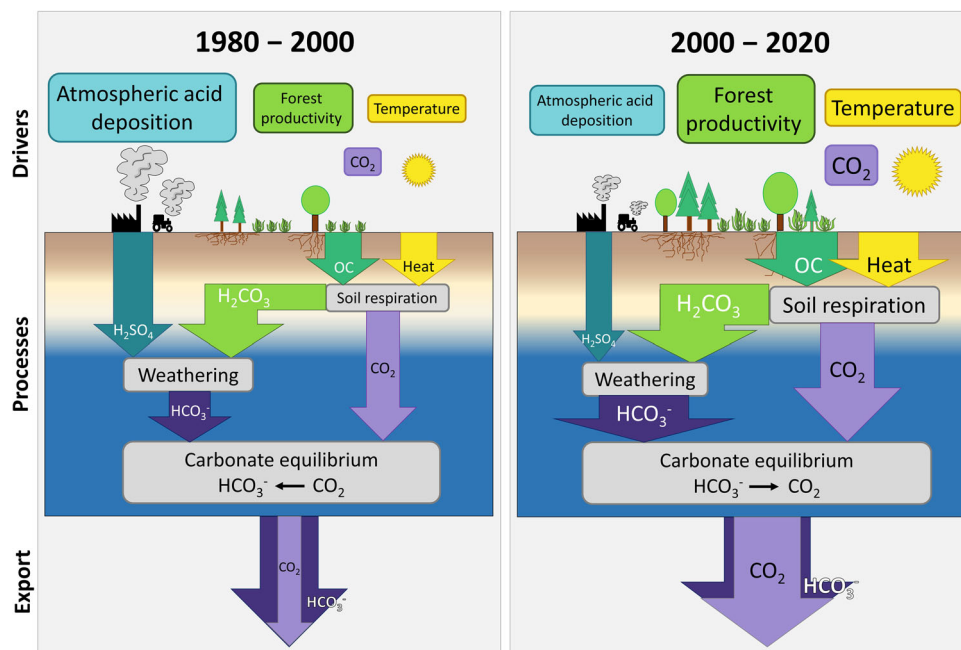
**Fig. 4 Conceptual diagram of hypothesized patterns and main drivers of decadal groundwater DIC trends.** Boxes show states or processes and arrows show fluxes. Symbol size scales qualitatively with concentration, process rate or flux. Patterns and drivers are considered typical for acid sensitive landscapes under the influence of reductions in atmospheric acid deposition. Reductions in atmospheric acid deposition shifts weathering pathways towards lower importance of sulfuric acid ($H_2SO_4$) relative to carbonic acid ($H_2CO_3$), leading to higher $HCO_3^-$ production in non-carbonate bedrock. Higher forest productivity and decreased atmospheric acid deposition may cause larger organic carbon (OC) supply and soil respiration, potentially further stimulated by climate warming and atmospheric $CO_2$ increase. $CO_2$ production from soil respiration contributes acidity and a shift in the carbonate equilibrium towards more $CO_2$ at the expense of $HCO_3^-$.

been rising by 22% during 1980–2020[22]. Fifth, warming may have stimulated soil organic carbon decomposition[39]. Swedish groundwater warmed indeed by 0.038 °C yr$^{-1}$, on average among sites (Supplementary Table 2, Supplementary Fig. 5), which could potentially have increased soil respiration by 10–26% (Supplementary Discussion 1).

Several alternative mechanisms could theoretically lead to changes in DIC but have likely minor influence here. For example, decreasing water levels would lead to a concentration of solutes through longer residence and reaction times and smaller water volumes. However, I did not find any significant change in water levels and no significant relationship between water levels and DIC among a subset of 15 sites with parallel water level and chemical measurements (Supplementary Fig. 8b, Supplementary Table 2). Moreover, liming applied in forestry, agriculture or water management adds $HCO_3^-$ and rises pH[17]. In Sweden, liming contributes on average 4% to riverine carbonates and has decreased substantially since 1980 and hence cannot explain a large-scale DIC increase[40]. Notwithstanding, the multitude of environmental changes that have taken place in Sweden during the past decades make it difficult to disentangle the contribution of single mechanisms and call for future more detailed mechanistic research.

**The dynamic role of groundwater in the contemporary C cycle.** Regardless of the exact driver, this unique four-decade long study reveals substantial changes in groundwater C cycling across a 450,000 km$^2$ region with diverse hydrogeological settings. These dynamics have important consequences for the role of groundwater in the contemporary C cycle. Whether groundwater is a sink or a source for atmospheric C has been debated for decades[1,3,14]. Traditionally, groundwater has been regarded as a global C sink over geologic time scales because more $CO_2$ is

consumed during silicate weathering than released during subsequent precipitation of the weathering products ($HCO_3^-$ and e.g. $Ca^{2+}$) as carbonate rock in oceans[1,3]. My findings challenge this view, because they indicate that elevated sulfuric acid inputs have caused an imbalance between $HCO_3^-$ and base cations (Fig. 3), which prevents carbonate rock formation and weakens the C sink over decadal time scales[18]. While these changes have started to reverse, they may take decades or centuries to recover because of an exhausted acid buffering capacity[26,27,29]. My findings also stress that the temporal evolution may depend on the hydrogeological settings, with somewhat more dynamic responses in shallower or unconfined relative to deeper or confined aquifers. Land use and climate changes may further modify the trajectories through their potential effects on soil respiration[14,37,39].

The C sink function of groundwater is also challenged by the emerging evidence that groundwater can act as a source for atmospheric C, because it contributes to a large extent to globally important C emissions from inland waters and C export to oceans[2,5,41,42]. An important question is to what extent rising groundwater DIC would propagate into C emissions from receiving surface waters. Indeed, DIC has been rising during the past decades in many diverse northern hemisphere surface waters, including Swedish waters[17,19,21,32,43–45], even if this was not the case everywhere[20,46,47]. In contrast, $CO_2$ concentrations have often not changed in the same pace or direction[20,47,48]. In Sweden, the mismatch in ground- and surface water $CO_2$ trends could be explained by the relatively short periods for which surface water $CO_2$ trends are available ($\leq$17 years)[48,49] relative to the time it may take for groundwater $CO_2$ changes to propagate to surface waters (~several decades)[50–52]. Alternatively, increased $CO_2$ export may be easily missed because $CO_2$ is quickly degassed to the atmosphere[42] or processed by metabolism in surface waters and these processes may have intensified[48]. Furthermore, changes in hydrological flow paths may have favored DIC over $CO_2$

export to surface waters[48,49]. Finally, riparian zones may have lost part of their capacity to enrich groundwater in $CO_2$ just before it discharges into surface waters[2,42], as a consequence of historic large-scale perturbations such as drainage ditching and maintanence[53]. This process is speculated to have contributed to declines in stream $CO_2$ concentrations across the USA over the past decades[47]. Collectively, my findings highlight the need of future research and monitoring efforts to unravel the hydrological and biogeochemical controls on C export from land to water in order to elucidate the role of changing groundwater DIC for surface water C emissions and C export to oceans. My findings also urge for investigations on the extent to which rising groundwater DIC mirrors an increased terrestrial net C uptake[6,14] or constitutes a net C source to surface waters and the atmosphere[7].

The changes in groundwater chemistry observed here are likely representative for many aquifers globally. A total of 7–17% of global land area has been acidified due to atmospheric deposition and poor buffering capacity[54]. Slow recovery from acidification is a typical feature of groundwater in these regions[29,55,56]. Nearly half of the continental land surface contains local and relatively shallow aquifers similar as in Sweden[57]. Many of these have relatively high groundwater recharge and shallow water tables and are located in areas where atmospheric acid deposition has been declining such as northern Europe, northeastern North-America and southeastern Asia[52,57]. Even groundwater in areas where atmospheric acid deposition is still rising may show DIC changes. However, DIC may also increase independent of atmospheric deposition history and sensitivity to acidification, as reported for well-buffered carbonate-rich aquifers in the USA[13,58]. Together these observations corroborate my findings that bedrock mineralogy was of relatively minor importance for variation in DIC trends among aquifers and that drivers other than atmospheric acid deposition can cause DIC changes.

Investigating the mechanisms of global C cycling remains a major scientific challenge, in particular the sources, pathways and fates of C as it moves across the land-water continuum[6,7]. This work demonstrates the large potential of groundwater to provide unique insights in C cycle mechanisms because of its tight connection with the often independently studied atmosphere, vegetation, soils, bedrock and surface waters. Hence, groundwater can be regarded as a sentinel and integrator of environmental changes over time scales of its residence time. Groundwater chemistry is monitored in many countries worldwide. While direct DIC measurements are usually absent and should be introduced in future monitoring, alkalinity, pH and temperature is typically monitored and can be useful to approximately track past and ongoing changes in surface C uptake and subsurface transformations, but potentially also as an early warning system of future changes in receiving surface waters. To predict these changes, it is crucial to accurately quantify the time scale and degree of connectivity at which environmental change effects on the land surface propagate through groundwater and surface waters[11]. Closer collaboration among hydrologists, hydrogeologists, limnologists, atmospheric scientists and soil scientists will be vital for the inclusion of groundwater in C budgets, the legacies it constitutes in the C cycle, and the wider effects it has on aquatic ecosystem functioning. Such efforts will not only help to better predict future landscape and global C fluxes, but also to develop integrated watershed management tools to improve water quality, C sequestration and climate change mitigation[2].

## Methods

**Data collection**. I explored groundwater chemistry data collected within the environmental monitoring program of the Swedish Geological Survey. In total, data was available from 1738 sampling sites for the period 1962–2020[59]. Here, I focus on the period 1980–2020 because sampling was greatly intensified in 1980 (Supplementary Fig. 2) and selected 55 sites with observations available for at least 65% of the total number of years in the period and at least two observations in the first and last four years of the period[60]. These sites are part of the national groundwater quality monitoring program and were specifically selected in areas free from local human impacts. Most sites had data for the full 41 year record and at least 32 years, with 60–180 observations per year distributed equally over the year (Supplementary Fig. 9). Sampling and sample analysis for these sites was done following standardized methods within the Swedish national groundwater monitoring program. Groundwater was extracted with various types of pumps or fetchers adapted to the specific sampling site. Generally, great care was taken to minimize gas exchange with the atmosphere during sampling. Samples were transported to accredited Swedish laboratories in cooling boxes and stored at 4 °C upon analysis (typically within <3 days). The laboratories were at Meteorological Institute (MISU), Stockholm University (until 1980), Geological Survey of Sweden, Uppsala (1980–1992), and Department of Aquatic Sciences and Assessment, Swedish University of Agricultural Sciences, Uppsala (since 1992). Field measurements included water temperature (T) and dissolved oxygen ($O_2$) concentrations. Laboratory measurements included pH, alkalinity, electrical conductivity, base cations ($Ca^{2+}$, $Mg^{2+}$, $K^+$, $Na^+$), acid anions ($SO_4^{2-}$, $Cl^-$, $NO_3^-$), ammonium ($NH_4^+$), dissolved silica ($SiO_2$), and total organic carbon concentrations (TOC, which can be assumed to be nearly identical to DOC)[19]. Samples for pH analysis were handled during transport and analysis (potentiometric pH meter) without direct contact with surrounding air in order to minimize disruption of the gas equilibrium. Alkalinity was measured using the Gran titration method (titration to pH 5.4) and is defined as the acid buffering capacity. Further details on analytical methods are available elsewhere[61] (Supplementary Table 5). Groundwater chemistry data was complemented by water level measurements available for a subset of 15 sites[62]. Level measurements and water sampling was not always performed on the same day and therefore matched with a tolerance of 14 days. Geographical data was available for each site and included information on latitude, longitude, depths of water intake in well, aquifer type (unconfined/confined) and bedrock type (silicate/carbonate). Bedrock type at site locations was derived from a geological map[63].

**Data preprocessing**. For each time series, I removed outliers defined as values beyond the median ± three times the standard deviation within a running window of ±10 values. This procedure removed <3% (median, <6% max) of all values for any variable. In a few cases, values were below the minimum detection limit of the respective measurement method[61]. This was the case for <0.1% of pH and alkalinity observations, 9% of $NO_3^-$ observations and 26% of $NH_4^+$ observations, as a median among sites. I set these values to random numbers between zero and the respective detection limits using a bootstrap approach (see section on 'uncertainty propagation' below). Hence, the $NO_3^-$ trends need to be treated with caution. $NH_4^+$ trends were not calculated because trends would be biased by variable detection limits (0.004–0.05 mg $L^{-1}$). $SiO_2$ trend calculations were also omitted due to reported issues with method changes[61]. Water temperature was missing in a few cases (9%) and was gap-filled using linear regression with 'year' and 'day of year' as predictors to account for decadal and seasonal trends. The median standard error of prediction was 0.22 °C (0.07–0.44) and had negligible effects on DIC and $CO_2$ calculations (<1%).

**DIC and $CO_2$ calculations**. I calculated DIC and $CO_2$ concentrations from measured pH, alkalinity and temperature based on well-established carbonate equilibrium equations[64]. I also calculated bicarbonate alkalinity ($HCO_3^-$), correcting measured alkalinity for other potential sources of alkalinity (e.g. silicates), except DOC (but see sensitivity analysis below). I performed the calculations using the geochemical modeling program PHREEQC version 3.7.5 developed by the US Geological Survey and implemented as an R package ('phreeqc')[65,66]. PHREEQC is commonly used in groundwater chemistry modeling and has also been used for large-scale and long-term assessments of C cycling where direct DIC or $CO_2$ measurements are typically not available[13,16]. PHREEQC simulates a variety of equilibrium reactions between solutes, solids and gases with potential additional effect on the carbonate system. Here, I account for the distribution of major geochemical species ($Ca^{2+}$, $Mg^{2+}$, $K^+$, $Na^+$, $SO_4^{2-}$, $Cl^-$, $NO_3^-$, and $SiO_2$). The effect of these species on calculated DIC, $CO_2$, and $HCO_3^-$ was typically <1%.

**Sensitivity analysis**. The DIC and $CO_2$ calculations may be biased under relatively low pH and alkalinity as well as high DOC[67]. For example, organic acids may bias calculations in high DOC waters because they also contribute to measured (Gran) alkalinity. Here, this contribution estimated for the period 2000–2020 following[68] (Supplementary Methods 1) was 1% as median among all sites and ≤8% in 90% of all sites. With such low contributions, even relatively large trends in DOC would likely cause only little bias in observed trends in alkalinity[69]. Another source of error lies in potential underestimation of pH in low ionic strength waters by certain types of potentiometric pH meters[70]. Corrections based on ionic strength estimated using measured concentrations of base cations, acid anions and alkalinity (Supplementary Methods 1)[70] suggest that pH values could be underestimated by 0.10 units as median among all sites. This, however, is a conservative maximum

estimate, because the pH measurements in this study rely on electrodes that are particularly adapted to minimize diffusion voltages that would cause under-estimation of pH in low ionic strength waters, following international standards (Supplementary Table 5). Alkalinity and pH corrections would reduce the calculated DIC and $CO_2$ concentrations and therefore also their absolute trends in 2000–2020 (−6 to −9% and −16 to −22%, respectively, Supplementary Table 4, Supplementary Fig. 10). However, the trends relative to median concentrations were not biased in any considerable way (+2 to +4% and −2 to −10%) and alkalinity and pH corrections balanced each other (Supplementary Table 4). Importantly, absolute and relative DIC and $CO_2$ trends remain highly significant among sites ($p < 0.001$) and the proportion of sites with significant increases or decreases was nearly unaffected (Supplementary Table 4). Furthermore, DIC and $CO_2$ trends were similar for different subsets of sites with pH and $HCO_3^-$ below and above critical thresholds that are generally associated with more or less biased estimates[67] (pH $\leq/>$ 6.5 and/or $HCO_3^-$ $\leq/>$ 1 mEq $L^{-1}$, Supplementary Fig. 11). Together, these analyses stress the robustness of the main results in this paper relative to errors in carbonate equilibrium estimations. Further support is provided by the fact that the DIC estimates in this study (Supplementary Fig. 1a) were of similar magnitude as direct DIC measurements in other Swedish groundwater sampling sites[12].

**Linear trend analysis**. I quantified decadal monotonic rates of change per unit time in the measured water quality parameters using the Theil–Sen estimator (referred to as 'trends' and the symbol Δ throughout the manuscript)[71]. This estimator is the median of the slopes resulting from all pairs of samples and is hence robust against outliers. To yield relative changes in % $yr^{-1}$, I divided trends by the median concentration for a given period and multiplied by 100. I evaluated the significance in trends using the seasonal Kendall test with corrections for serial dependence[72]. The seasonal Kendall test calculates a trend for each season (spring = March–May, summer = June–August, autumn = September–November, winter = December–February) and combines season-specific trends to test for an overall trend. This approach has been widely used to test for trends in water quality[13,20,48]. I performed the trend analyses using the "rkt" function of the "rkt" package for the statistical program R 3.6.1[73,74]. The function allows for correction of test statistics for correlation between seasons. The corrections never had any noteworthy effect on test statistics but required substantial computation time. I therefore disabled the corrections in the final analysis. In very few cases (<1% of all data), sites were sampled repeatedly within 3 days. I averaged values from such consecutive samplings, because they would otherwise considerably slow down computation times for trend analyses. I evaluated the overall trend among all sites using the two-tailed Student's $t$-test with the null hypothesis of h0: mean = 0 using the "t.test" function in R. In these tests spatial autocorrelation was never an issue, as indicated by non-significant correlation coefficients Moran's I ($p > 0.05$), calculated using the "calculatePvalue" function of the R package "Irescale"[75].

**Change point analysis**. To account for the possibility of non-monotonic trends in water chemistry that can be expected during recovery from acidification[27], I evaluated for each site the presence of a change point, i.e., a point in time when the local linear trend changed significantly in slope. Change points were identified using the "segmented" function of the R package "segmented"[76]. Change points were considered significant if a bi-linear model fitted the time series significantly better than a linear model, according to the likelihood ratio test performed using the "lr.test" function of the R package "lmtest"[77]. To visualize overall trends, I plotted observations from all sites against time, normalized to the respective site-specific median, accompanied by local quantile regressions (median and 90% percentiles). Local quantile regressions were calculated using 2nd order polynomial regressions ("loess" function in R package "stats", degree of smoothing = 0.75) fitted to rolling quantiles with a window size of 20 observations ("rollapply" function in R package "zoo"[78] applied to "quantile" function in R package "stats"[74]).

**Multivariate statistics**. I evaluated potential drivers of DIC and $CO_2$ trends among sites ($n = 55$) using two sets of multiple linear regressions, including relevant water chemical and geographical predictor variables. In water chemical models, I regressed the trends of DIC, $CO_2$, $H^+$ and $HCO_3^-$, respectively, against the trends of base cations, acid anions, and water temperature. In geographical models, I regressed the trends of DIC, $CO_2$, $H^+$ and $HCO_3^-$, respectively, against latitude, depth of water intake in well (hereafter referred to as 'well depth'), aquifer type and bedrock type as predictor variables. I set 'well depth' to 0 m for springs. For each set of models, I selected the most parsimonious model from a suite of candidates fitted based on all possible combinations of predictor variables and ranked using Akaike's Information Criterion. I selected the most parsimonious model using the "dredge" function in the R package "MuMIn"[79]. I fitted the water chemical models using robust linear regression and the MM estimator by means of the "rlm" function in R. Robust regression downweighs the influence of outliers and is recommended for models with compositional water chemical data (Supplementary Methods 2). Outliers were no issue in the geographical models which is why I fitted them using ordinary least square regression by means of the "lm" function in R. In all models, multicollinearity among predictor variables was minor

because variance inflation factors calculated using the "vif" function of the R package "car"[80] were always <4 and typically <2. Furthermore, spatial auto-correlation was never an issue, as suggested by comparisons of models with and without accounting for correlation structure (exponential relationship with latitude + longitude). These models were fitted using the "gls" function in R and compared using the likelihood ratio test ($p > 0.05$) and the "lr.test" function of the R package "lmtest"[77].

**Data transformation**. In multivariate analysis, it is important to account for the compositional nature of water chemical data. The use of raw concentration data may result in problems such as spurious correlations and incorrect interpretation. To avoid these problems in the water chemical models, I transformed all water chemical variables to so-called Pivot log-ratio coordinates (plr) using the R package 'robCompositions'[81] (see Supplementary Methods 2 for details). To approximately conform to normality assumptions in Student's $t$-tests and multivariate geographical models, I transformed variables if needed and report back-transformed statistics for $t$-tests. I used either $\log_{10}(X + 1)$ or $asinh(a \cdot X)$-transformation of variable X, where $a$ was between 10 and 10000. For pH, I base all statistics on the activity of the hydrogen ion, $H^+ = 10^{-pH}$, and report results based on back-transformed pH values, where possible. In particular, I calculated temporal trends as $\Delta pH = -\log_{10}(\tilde{H^+} + \frac{1}{2}\Delta H^+) - -\log_{10}(\tilde{H^+} - \frac{1}{2}\Delta H^+)$, where $\Delta pH$ and $\Delta H^+$ are the Theil–Sen slopes of pH and $H^+$, respectively, and $\tilde{H^+}$ is the median of $H^+$.

**Uncertainty propagation**. I propagated analytical uncertainties in input variables in their effect on trends using a parametric bootstrap approach[82]. For each sampling site, I resampled each observation 500 times from standard probability distributions defined by the mean and standard deviation of the analytical estimates as reported by the laboratory[61] (Supplementary Table 5), as reported by the literature (organic matter contribution to alkalinity, Supplementary Methods 1), or as predicted by the water temperature gap filling model (see 'Data preprocessing'). I assumed the error in water level measurements and geographical variables to be negligible. The distribution I sampled from were normal (T), log-normal (pH) or gamma (all other variables). In particular, I replaced values below the detection limit by a sample from a uniform distribution bound by zero and the detection limit. I calculated temporal trends for each of the 500 randomly created time series. I performed all statistical analyses on each of the 500 bootstrapped trends and summarized the resulting distribution of test statistics by means and 95% percentiles (which yield confidence intervals).

## Data availability
All raw data used in this paper are openly available through the Swedish Geological Survey[59,62]. All variables calculated from raw data are available open access through the Swedish National Data Service[83]. Source data as well as Supplementary Tables 1–4 are available through Hydroshare[84].

## Code availability
R code for statistical analyses and generation of figures and tables is provided upon request.

## References
1. Monger, C. H. et al. Sequestration of inorganic carbon in soil and groundwater. *Geology* **43**, 375–378 (2015).
2. Duvert, C., Butman, D. E., Marx, A., Ribolzi, O. & Hutley, L. B. $CO_2$ evasion along streams driven by groundwater inputs and geomorphic controls. *Nat. Geosci.* **11**, 813–818 (2018).
3. Kessler, T. J. & Harvey, C. F. The global flux of carbon dioxide into groundwater. *Geophys. Res. Lett.* **28**, 279–282 (2001).
4. Cole, J. J. & Prairie, Y. T. Dissolved $CO_2$ in freshwater systems. *Ref. Modul. Earth Syst. Environ. Sci.* https://doi.org/10.1016/b978-0-12-409548-9.09399-4 (2014).
5. Drake, T. W., Raymond, P. A. & Spencer, R. G. M. Terrestrial carbon inputs to inland waters: a current synthesis of estimates and uncertainty. *Limnol. Oceanogr. Lett.* **3**, 132–142 (2018).
6. Ballantyne, A. P., Alden, C. B., Miller, J. B., Trans, P. P. & White, J. W. C. Increase in observed net carbon dioxide uptake by land and oceans during the past 50 years. *Nature* **488**, 70–73 (2012).
7. Regnier, P. et al. Anthropogenic perturbation of the carbon fluxes from land to ocean. *Nat. Geosci.* **6**, 597–607 (2013).

8. Butman, D. E., Wilson, H. F., Barnes, R. T., Xenopoulos, M. A. & Raymond, P. A. Increased mobilization of aged carbon to rivers by human disturbance. *Nat. Geosci.* **8**, 112–116 (2015).

9. Hensgens, G., Laudon, H., Johnson, M. S. & Berggren, M. The undetected loss of aged carbon from boreal mineral soils. *Sci. Rep.* **11**, 1–10 (2021).

10. McDonough, L. K. et al. Changes in global groundwater organic carbon driven by climate change and urbanization. *Nat. Commun.* **11**, 1–10 (2020).

11. Zhang, S. & Planavsky, N. J. Revisiting groundwater carbon fluxes to the ocean with implications for the carbon cycle. *Geology* **48**, 67–71 (2020).

12. Nydahl, A. C., Wallin, M. B., Laudon, H. & Weyhenmeyer, G. A. Groundwater carbon within a boreal catchment: spatiotemporal variability of a hidden aquatic carbon pool. *J. Geophys. Res. Biogeosci.* **125**, 1–15 (2020).

13. Macpherson, G. L. et al. Increasing shallow groundwater $CO_2$ and limestone weathering, Konza Prairie, USA. *Geochim. Cosmochim. Acta* **72**, 5581–5599 (2008).

14. Andrews, J. A. & Schlesinger, W. H. Soil $CO_2$ dynamics, acidification, and chemical weathering in a temperature forest with experimental $CO_2$ enrichment. *Global Biogeochem. Cycles* **15**, 149–162 (2001).

15. Sánchez-Cañete, E. P., Barron-Gafford, G. A. & Chorover, J. A considerable fraction of soil-respired $CO_2$ is not emitted directly to the atmosphere. *Sci. Rep.* **8**, 2–11 (2018).

16. Macpherson, G. L. $CO_2$ distribution in groundwater and the impact of groundwater extraction on the global C cycle. *Chem. Geol.* **264**, 328–336 (2009).

17. Stets, E. G., Kelly, V. J. & Crawford, C. G. Long-term trends in alkalinity in large rivers of the conterminous US in relation to acidification, agriculture, and hydrologic modification. *Sci. Total Environ.* **488–489**, 280–289 (2014).

18. Das, S. et al. The role of sulfuric acid in continental weathering: insights from dissolved major ions and inorganic carbon isotopes of the Teesta River, Lower Brahmaputra System. *Geochem. Geophys. Geosyst.* **22**, 1–15 (2021).

19. Garmo, Ø. A. et al. Trends in surface water chemistry in acidified areas in Europe and North America from 1990 to 2008. *Water. Air. Soil Pollut.* **225**, 1–14 (2014). **1880**.

20. Seekell, D. A. & Gudasz, C. Long-term $pCO_2$ trends in Adirondack Lakes. *Geophys. Res. Lett.* **43**, 5109–5115 (2016).

21. Futter, M. N., Valinia, S., Löfgren, S., Köhler, S. J. & Fölster, J. Long-term trends in water chemistry of acid-sensitive Swedish lakes show slow recovery from historic acidification. *Ambio* **43**, 77–90 (2014).

22. Tans, P. & Keeling, R. Trends in atmospheric carbon dioxide. https://gml.noaa.gov/ccgg/trends/ (2022).

23. von Brömssen, U. Acidification Trends in Swedish Groundwaters. Review of time series 1950-85. National Swedish Environmental Protection Board Report 3547 (1989).

24. Löfgren, S. et al. Recovery of soil water, groundwater, and streamwater from acidification at the swedish integrated monitoring catchments. *Ambio* **40**, 836–856 (2011).

25. Ferm, M. et al. Wet deposition of ammonium, nitrate and non-sea-salt sulphate in Sweden 1955 through 2017. *Atmos. Environ. X* **2**, 100015 (2019).

26. Knutsson, G. et al. Acidification of groundwater in forested till areas. *Ecol. Bull.* **44**, 271–300 (1995).

27. Galloway, J. N., Norton, S. A. & Church, M. R. Freshwater acidification from atmospheric deposition of sulfuric acid. *Environ. Sci. Technol.* **17**, 541–545 (1983).

28. Akselsson, C., Hultberg, H., Karlsson, P. E., Pihl Karlsson, G. & Hellsten, S. Acidification trends in south Swedish forest soils 1986–2008 - Slow recovery and high sensitivity to sea-salt episodes. *Sci. Total Environ.* **444**, 271–287 (2013).

29. Caritat, P. D. E. & Kirkhusmo, L. A. The Norwegian groundwater monitoring network (LGN): alkalinity trends in selected aquifers from southern Norway during 1980–1990. *NGU Bull.* **427**, 79–82 (1995).

30. Karltun, E., Stendahl, J., Iwald, J. & Löfgren, S. Forest biomass accumulation is an important source of acidity to forest soils: data from Swedish inventories of forests and soils 1955 to 2010. *Ambio* **51**, 199–208 (2022).

31. Norton, S. A., Cosby, B. J., Fernandez, I. J., Kahl, J. S. & Church, M. R. Long-term and seasonal variations in $CO_2$: Linkages to catchment alkalinity generation. *Hydrol. Earth Syst. Sci.* **5**, 83–91 (2001).

32. Couturier, M., Prairie, Y. T., Paterson, A. M., Emilson, E. J. S. & del Giorgio, P. A. Long-term trends in $pCO_2$ in lake surface water following rebrowning. *Geophys. Res. Lett.* **49**, 1–9 (2022).

33. Janssens, I. A. et al. Reduction of forest soil respiration in response to nitrogen deposition. *Nat. Geosci.* **3**, 315–322 (2010).

34. Olsson, P., Linder, S., Giesler, R. & Högberg, P. Fertilization of boreal forest reduces both autotrophic and heterotrophic soil respiration. *Glob. Chang. Biol.* **11**, 1745–1753 (2005).

35. Meng, C. et al. Global soil acidification impacts on belowground processes. *Environ. Res. Lett.* **14**, 074003 (2019).

36. Cai, W.-J., Wang, Y., Krest, J. & Moore, W. S. The geochemistry of dissolved inorganic carbon in a surficial groundwater aquifer in North Inlet, South Carolina, and the carbon fluxes to the coastal ocean. *Geochim. Cosmochim. Acta* **67**, 631–637 (2003).

37. Janssens, I. A. et al. Productivity overshadows temperature in determining soil and ecosystem respiration across European forests. *Glob. Chang. Biol.* **7**, 269–278 (2001).

38. Nilsson, P., Roberge, C., Dahlgren, J. & Fridman, J. Forest statistics 2022. Official Statistics of Sweden Swedish University of Agricultural Sciences Umeå 2022 (2022).

39. Davidson, E. A. & Janssens, I. A. Temperature sensitivity of soil carbon decomposition and feedbacks to climate change. *Nature* **440**, 165–173 (2006).

40. Humborg, C. et al. $CO_2$ supersaturation along the aquatic conduit in Swedish watersheds as constrained by terrestrial respiration, aquatic respiration and weathering. *Glob. Chang. Biol* **16**, 1966–1978 (2010).

41. Weyhenmeyer, G. A. et al. Significant fraction of $CO_2$ emissions from boreal lakes derived from hydrologic inorganic carbon inputs. *Nat. Geosci.* **8**, 933–936 (2015).

42. Leith, F. I. et al. Carbon dioxide transport across the hillslope-riparian-stream continuum in a boreal headwater catchment. *Biogeosciences* **12**, 1881–1902 (2015).

43. Raymond, P. A. & Cole, J. J. Increase in the export of alkalinity from North America's largest river. *Science* **301**, 88–91 (2003).

44. Müller, J. D., Schneider, B. & Rehder, G. Long-term alkalinity trends in the Baltic Sea and their implications for $CO_2$-induced acidification. *Limnol. Oceanogr.* **61**, 1984–2002 (2016).

45. Räike, A., Kortelainen, P., Mattsson, T. & Thomas, D. N. Long-term trends (1975–2014) in the concentrations and export of carbon from Finnish rivers to the Baltic Sea: organic and inorganic components compared. *Aquat. Sci.* **78**, 505–523 (2016).

46. Finlay, K. et al. Decrease in $CO_2$ efflux from northern hardwater lakes with increasing atmospheric warming. *Nature* **519**, 215–218 (2015).

47. Jones, J. B., Stanley, E. H. & Mulholland, P. J. Long-term decline in carbon dioxide supersaturation in rivers across the contiguous United States. *Geophys. Res. Lett.* **30**, 1495 (2003).

48. Nydahl, A. C., Wallin, M. B. & Weyhenmeyer, G. A. No long-term trends in $pCO_2$ despite increasing organic carbon concentrations in boreal lakes, streams, and rivers. *Global Biogeochem. Cycles* **31**, 985–995 (2017).

49. Rehn, L., Sponseller, R., Laudon, H. & Marcus, W. Long-term changes in dissolved inorganic carbon (DIC) across boreal streams caused by altered hydrology. *Limnol. Oceanogr.* **68**, 409–423 (2023).

50. Kolbe, T., Marçais, J., de Dreuzy, J. R., Labasque, T. & Bishop, K. Lagged rejuvenation of groundwater indicates internal flow structures and hydrological connectivity. *Hydrol. Process.* **34**, 2176–2189 (2020).

51. Åkesson, M. et al. Constraining age distributions of groundwater from public supply wells in diverse hydrogeological settings in Scania, Sweden. *J. Hydrol.* **528**, 217–229 (2015).

52. Gleeson, T., Befus, K. M., Jasechko, S., Luijendijk, E. & Cardenas, M. B. The global volume and distribution of modern groundwater. *Nat. Geosci.* **9**, 161–164 (2016).

53. Ecke, F. Drainage ditching at the catchment scale affects water quality and macrophyte occurrence in Swedish lakes. *Freshw. Biol* **54**, 119–126 (2009).

54. Bouwman, A. F., Van Vuuren, D. P., Derwent, R. G. & Posch, M. A global analysis of acidification and eutrophication of terrestrial ecosystems. *Water. Air. Soil Pollut.* **141**, 349–382 (2002).

55. Edmunds, W. M. & Kinniburgh, D. G. The susceptibility of UK groundwaters to acidic deposition. *J. Geol. Soc. London* **143**, 707–720 (1986).

56. Taylor, F. B. & Symom, G. E. Effects of acid rain on water supplies in the Northeast. *J. Am. Water Work. Assoc.* **76**, 34–41 (1984).

57. Richts, A., Struckmeier, W. F. & Zaepke, M. WHYMAP and the Groundwater Resources Map of the World 1:25,000,000. in *Sustaining Groundwater Resources* (ed. Jones, J. A. A.) 159–173 (Springer, 2011).

58. Kent, R. & Landon, M. K. Triennial changes in groundwater quality in aquifers used for public supply in California: utility as indicators of temporal trends. *Environ. Monit. Assess.* **188**, 610 (2016).

59. Swedish Geological Survey (SGU). Data från miljöövervakning av grundvatten, öppna data (Groundwater environmental monitoring data, in Swedish). https://www.sgu.se/produkter/geologiska-data/oppna-data/grundvatten-oppna-data/miljoovervakning-av-grundvatten/ (2022).

60. De Wit, H. A. et al. Cleaner air reveals growing influence of climate on dissolved organic carbon trends in northern headwaters. *Environ. Res. Lett.* **16**, 104009 (2021).

61. SLU. Geochemical laboratory. Department of Aquatic Sciences and Assessment. Swedish University of Agricultural Sciences. https://www.slu.se/en/departments/aquatic-sciences-assessment/laboratories/vattenlabb2/ (2022).

62. Swedish Geological Survey (SGU). Data om grundvattennivåer (Groundwater level data, in Swedish). https://www.sgu.se/grundvatten/grundvattennivaer/ladda-ned-grundvattendata/ (2022).

63. Swedish Geological Survey (SGU). Berggrund 1:1 miljon (Bedrock Sweden 1:1 Million, in Swedish). https://apps.sgu.se/kartvisare/kartvisare-berggrund-1-miljon.html (2010).

r

ARTICLE

e

COMMUNICATIONS EARTH & ENVIRONMENT

t

s

g

...

64. Stumm, W. & Morgan, J. J. *Aquatic Chemistry: Chemical Equilibria and Rates in Natural Waters*, 3rd edn. (John Wiley & Sons, 1995).

65. Parkhurst, D. L. & Appelo, C. A. J. Description of input and examples for PHREEQC version 3—A computer program for speciation, batch-reaction, one-dimensional transport, and inverse geochemical calculations. in U.S. Geological Survey Techniques and Methods, book 6, chap. A43, 497 p., https://pubs.usgs.gov/tm/06/a43/ (2013).

66. Charlton, S. R. & Parkhurst, D. Modules based on the geochemical model PHREEQC for use in scripting and programming languages. *Comput. Geosci.* **37**, 1653–1663 (2011).

67. Abril, G. et al. Technical note: Large overestimation of $pCO_2$ calculated from pH and alkalinity in acidic, organic-rich freshwaters. *Biogeosciences* **12**, 67–78 (2015).

68. Lydersen, E., Larssen, T. & Fjeld, E. The influence of total organic carbon (TOC) on the relationship between acid neutralizing capacity (ANC) and fish status in Norwegian lakes. *Sci. Total Environ.* **326**, 63–69 (2004).

69. Skjelkvåle, B. L., Borg, H., Hindar, A. & Wilander, A. Large scale patterns of chemical recovery in lakes in Norway and Sweden: importance of seasalt episodes and changes in dissolved organic carbon. *Appl. Geochem.* **22**, 1174–1180 (2007).

70. Liu, S., Butman, D. E. & Raymond, P. A. Evaluating CO2 calculation error from organic alkalinity and pH measurement error in low ionic strength freshwaters. *Limnol. Oceanogr. Methods* **18**, 606–622 (2020).

71. Sen, P. K. On a class of aligned rank order tests in two-way layouts. *Ann. Math. Stat.* **39**, 1115–1124 (1968).

72. Hirsch, R. M. & Slack, J. R. A nonparametric trend test for seasonal data with serial dependence. *Water Resour. Res.* **20**, 727–732 (1984).

73. Marchetto, A. rkt: Mann-Kendall Test, Seasonal and Regional Kendall Tests. R package version 1.6. https://CRAN.R-project.org/package=rkt (2021).

74. R Development Core Team. R: A language and environment for statistical computing. R Foundation for Statistical Computing, Vienna, Austria. http://www.R-project.org (2019).

75. Fuentes, I., DeWitt, T., Ioerger, T. & Bishop, M. Irescale: Calculate and Rectify Moran's I. R package version 2.3.0. https://CRAN.R-project.org/package=Irescale (2019).

76. Muggeo, V. M. R. segmented: an R Package to Fit Regression Models with Broken-Line Relationships. R News, 8/1, 20–25. https://cran.r-project.org/doc/Rnews/ (2008).

77. Zeileis, A. & Hothorn, T. Diagnostic checking in regression relationships. *R News* **2**, 7–10 (2002).

78. Zeileis, A. & Grothendieck, G. Zoo: S3 infrastructure for regular and irregular time series. *J. Stat. Softw.* **14**, 1–27 (2005).

79. Barton, K. MuMIn: Multi-Model Inference. R package version 1.43.6. https://CRAN.R-project.org/package=MuMIn (2019).

80. Fox, J. & Weisberg, S. *An {R} Companion to Applied Regression*, Third Edition. Thousand Oaks CA: Sage. https://socialsciences.mcmaster.ca/jfox/Books/Companion/ (2019).

81. Templ M., Hron K., Filzmoser P. robCompositions: an R-package for robust statistical analysis of compositional data. v. 2.3.1. in *Compositional Data Analysis. Theory and Applications* (eds. Pawlowsky-Glahn, V. & Buccianti, A.) 341–355 (John Wiley & Sons, 2011).

82. Soderberg, K. & Hennet, R. J.-C. Uncertainty and trend analysis. radium in ground water and drinking water. *Groundw. Monit. Remediat.* **27**, 122–129 (2007).

83. Klaus, M. Trends in groundwater chemistry across Sweden during 1980−2020. Swedish National Data Service. Version 1. https://doi.org/10.5878/ms33-dh85 (2023).

84. Klaus, M. Supplementary Tables and Source Data for 'Decadal increase in groundwater inorganic carbon concentrations across Sweden', HydroShare, http://www.hydroshare.org/resource/8ea572a2615c404f8e441e35286829f1 (2023).

## Author contributions
M.K. conceived the study, performed all analyses and wrote the manuscript.

## Competing interests
The author declares no competing interests.

## Additional information
**Supplementary information** The online version contains supplementary material available at https://doi.org/10.1038/s43247-023-00885-4.

**Correspondence** and requests for materials should be addressed to Marcus Klaus.

**Peer review information** *Communications Earth & Environment* thanks Gwendolyn Macpherson, Eric Rosa and the other, anonymous, reviewer(s) for their contribution to the peer review of this work. Primary Handling Editors: Rahim Barzegar and Clare Davis. A peer review file is available.

**Reprints and permission information** is available at http://www.nature.com/reprints

**Publisher's note** Springer Nature remains neutral with regard to jurisdictional claims in published maps and institutional affiliations.